

## Supporting Information

### **A New Approach to Polycyclic Azaarenes: Visible-light Photolysis of Vinyl Azides in the Synthesis of Diazabenzopyrene and Diazaperylene.**

*Julia A. Schneider, Dmitrii F. Perepichka\**

\*McGill University, Department of Chemistry, 801 Sherbrooke Street West, H3A 0B8, QC,  
Montreal, Canada.

#### **Table of contents**

Additional spectroscopy & cyclic voltammetry & calculations	Page 2-4
Experimental Section	Page 5
NMR Data	Pages 6-14
Computational data	Pages 16-21

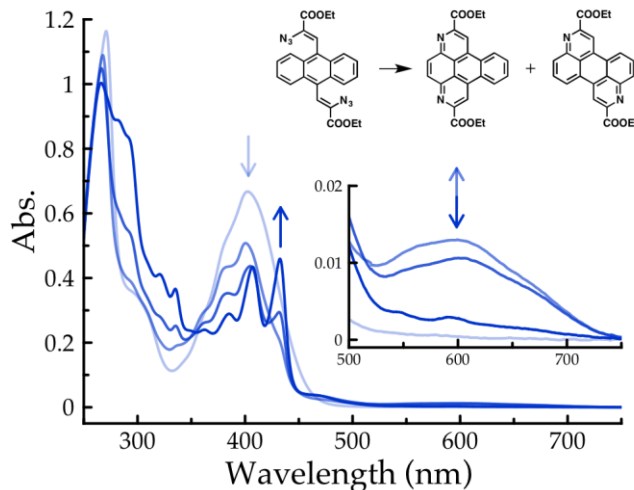


**Figure S1.** The absorption spectra showing the photocyclization of **5** at room temperature under ambient lighting. The broad peak of **5** is replaced by the sharper vibronic bands of cyclized **6** and **7**. The inset shows the appearance and disappearance of intermediate absorption signals.

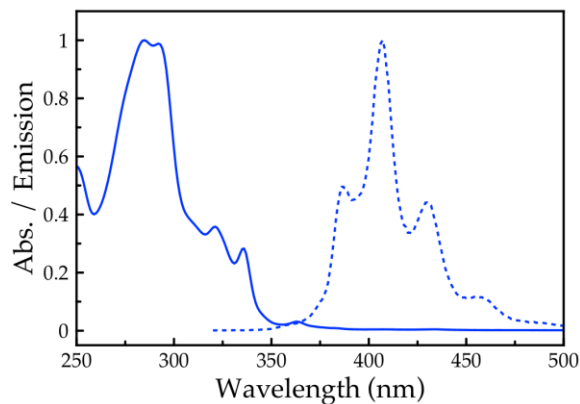


**Figure S2.** Absorption (—) and emission (- -) spectra of **6** in  $\text{CH}_2\text{Cl}_2$ ;  $\lambda^{\text{exc}} = 300 \text{ nm}$ .

**Table S1.** Ratios of isomers **6** and **7** in relation to the temperature of the photocyclization reaction.

Temperature	Loading	Crude yield	<b>6</b> : <b>7</b> Ratio
RT	0.10 g in 50 mL $\text{CH}_2\text{Cl}_2$	98%	62:38
-20 °C	0.50 g in 100 mL $\text{CH}_2\text{Cl}_2$	+100%	50:50
-50 °C	0.30 g in 100 mL $\text{CH}_2\text{Cl}_2$	+100%	42:58
-80 °C	0.015 g in 4 mL $\text{CH}_2\text{Cl}_2$	n/a	38:62

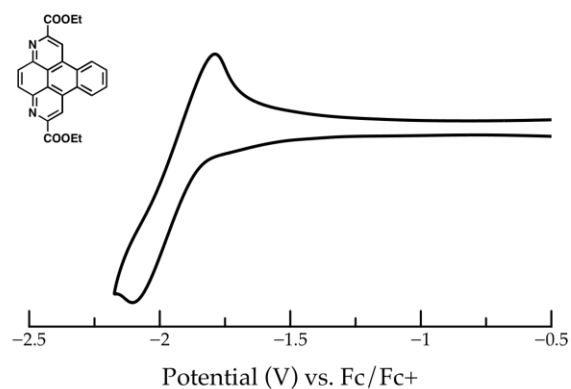


**Figure S3.** Cyclic voltammetry of **6** ( $\text{CH}_2\text{Cl}_2/0.1\text{M TBAPF}_6$ ).

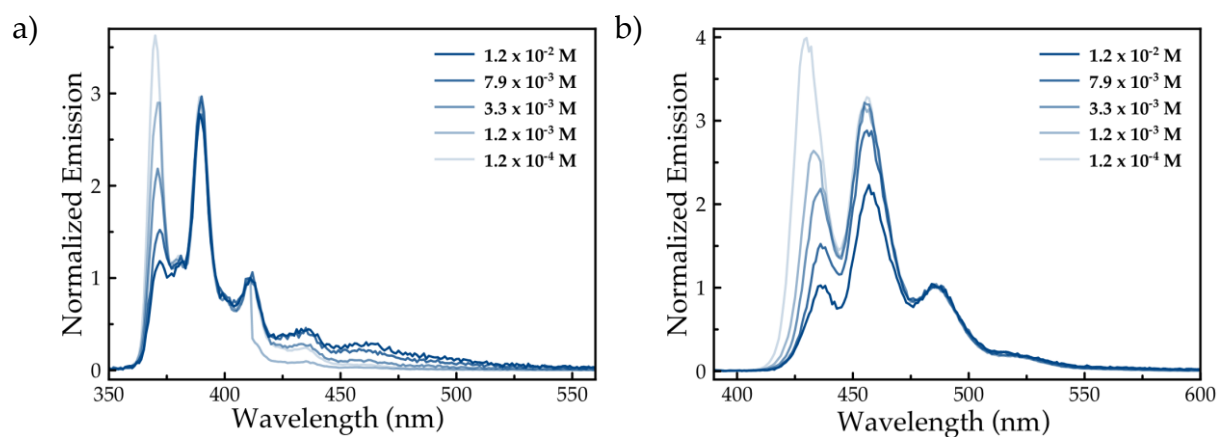


**Figure S4.** Emission spectra of **10** (a) and **11** (b) in increasing concentrations and normalized to the third emission band. The observed changes in the relative intensities of the vibronic bands can be explained by self-absorption.

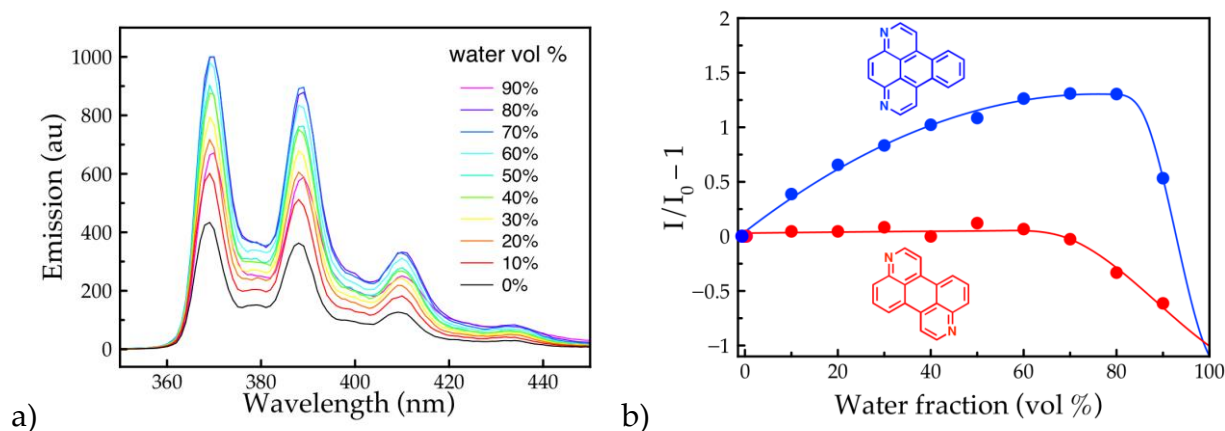


Figure S5. a) Emission spectra of 10 in MeCN-water solutions show polarity-induced enhanced emission. b) Plot of variations in PL peak intensities of 10 and 11 versus water fraction.

**Table S2.** Calculated transitions by TD-DFT.

	Transition	Orbitals	Wavelength (nm)	Oscillator strength
<b>10</b>	$S_0 \rightarrow S_1$	HOMO-1 $\rightarrow$ LUMO+1 HOMO-1 $\rightarrow$ LUMO+2 HOMO $\rightarrow$ LUMO	325.3	0.128
	$S_0 \rightarrow S_2$	HOMO-3 $\rightarrow$ LUMO+1 HOMO-2 $\rightarrow$ LUMO	311.1	0.002
	$S_1 \rightarrow S_0^a$	LUMO+1 $\rightarrow$ HOMO-1 LUMO+2 $\rightarrow$ HOMO-1 LUMO $\rightarrow$ HOMO	340.2	0.116
<b>11</b>	$S_0 \rightarrow S_1$	HOMO $\rightarrow$ LUMO	410.6	0.3403
	$S_1 \rightarrow S_0^a$	LUMO $\rightarrow$ HOMO	457.7	0.3423

a)  $S_1 \rightarrow S_0$  transitions calculated by re-optimizing the geometry of the excited state with TD-DFT (B3LYP/6-31d(d)).

## Experimental Section

UV/Vis absorption and photoluminescence spectra were measured in CH<sub>2</sub>Cl<sub>2</sub> with a JACSO V670 UV-Vis-NIR spectrometer and a Varian Eclipse Fluorimeter, respectively. The fluorescence quantum yields were determined relative to anthracene in EtOH ( $\Phi = 0.27$ ). Solid state fluorescence was acquired for powders on a FluoroLog-3 spectrofluorometer (Horiba Jobin Yvon Inc.).

Cyclic voltammetry was performed on a CH670 potentiostat from CH-Instruments in a three-electrode cell using a 0.1M TBAPF<sub>6</sub> electrolyte solution in acetonitrile, tetrahydrofuran or CH<sub>2</sub>Cl<sub>2</sub>, at scan rates of 100 mV s<sup>-1</sup>. Pt wire was used as the working and counter electrodes and a Ag/AgCl electrode as reference. All potentials were adjusted vs. ferrocene (internal standard).

Geometries, molecular orbital energies, and electronic transitions were calculated at the B3LYP/6-31G(d) level of theory using the Gaussian 09W program.<sup>11</sup> Frequency calculations were done for all optimized geometries, confirming these as energy minima.

## Synthetic procedures of known compounds

*Ethyl 2-azidoacetate* (**Warning: Small azide derivatives are potentially explosive. Reaction and isolation performed behind blast shield.**) Ethyl chloroacetate (10 mL, 0.093 mol) in EtOH (40 mL) was cooled to 0 °C in an ice bath. Sodium azide (7.0 g, 0.11 mol) was weighed out, dissolved in H<sub>2</sub>O (20 mL) and added to the cold reaction mixture. The solution was stirred at 0 °C for 20 minutes before being brought to reflux for 4.5 hrs. After cooling, the reaction mixture was washed with H<sub>2</sub>O (60 mL) and extracted with Et<sub>2</sub>O (3 × 50 mL). The combined organic layers were washed with H<sub>2</sub>O (3 × 50 mL), dried over Na<sub>2</sub>SO<sub>4</sub>, and the solvent was removed in vacuo to afford a clear oil (11.0 g, 95% yield), which was stored in a freezer. NMR data was in agreement with literature.<sup>2</sup> <sup>1</sup>H NMR (CDCl<sub>3</sub>, 500 MHz, 25°C)  $\delta$  4.29 (q, J = 7.2 Hz, 2H), 3.88 (s, 2H), 1.34 (t, J = 7.2 Hz, 3H). <sup>13</sup>CNMR (CDCl<sub>3</sub>, 125 MHz, 25°C)  $\delta$  168.3, 61.8, 50.3, 14.04.

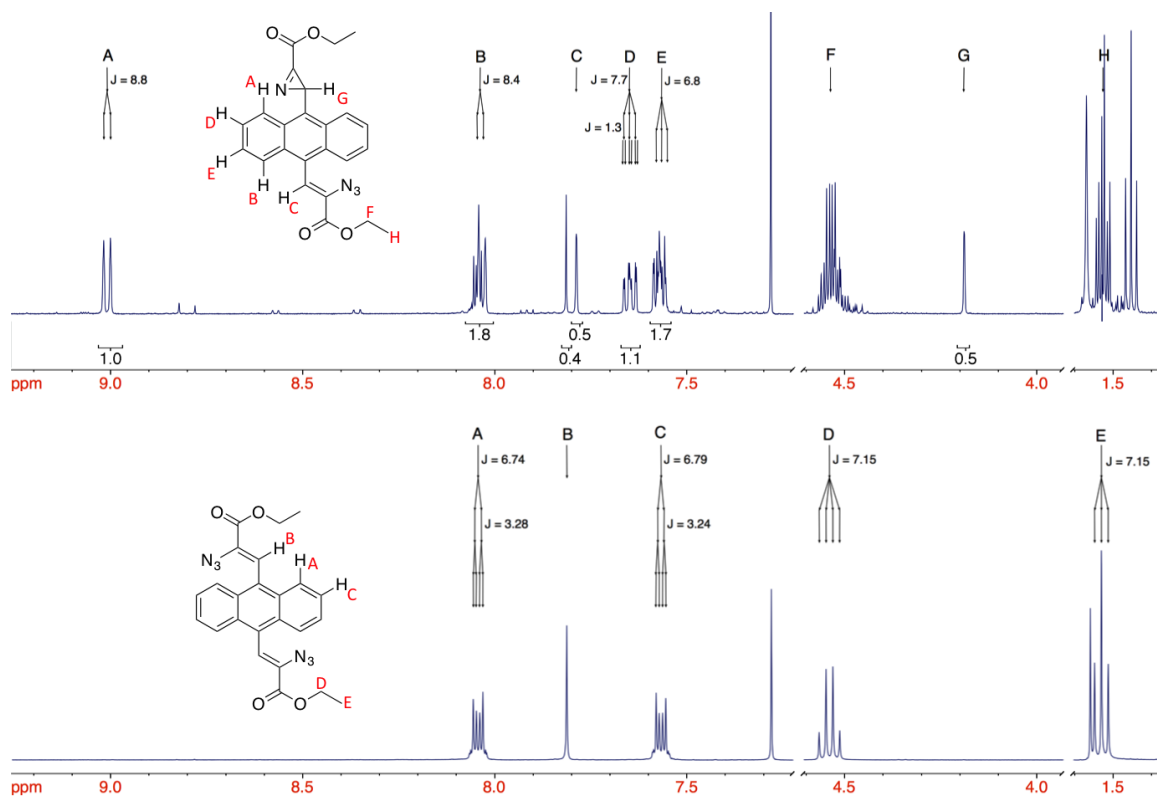
*Anthracene-9,10-dicarbaldehyde* (**4**) In a dry flask, 2.5 M n-butyllithium in hexane (19 mL, 0.13 mol) was added dropwise to a solution of 9,10-dibromoanthracene (6.4 g, 19

---

<sup>1</sup> Frisch, M. J.; Trucks, G. W.; Schlegel, H. B.; Scuseria, G. E.; Robb, M. A.; Cheeseman, J. R.; Scalmani, G.; Barone, V.; Mennucci, B.; Petersson, G. A.; Nakatsuji, H.; Caricato, M.; Li, X.; Hratchian, H. P.; Izmaylov, A. F.; Bloino, J.; Zheng, G.; Sonnenberg, J. L.; Hada, M.; Ehara, M.; Toyota, K.; Fukuda, R.; Hasegawa, J.; Ishida, M.; Nakajima, T.; Honda, Y.; Kitao, O.; Nakai, H.; Vreven, T.; Montgomery, J. A.; Peralta, J. E.; Ogliaro, F.; Bearpark, M.; Heyd, J. J.; Brothers, E.; Kudin, K. N.; Staroverov, V. N.; Kobayashi, R.; Normand, J.; Raghavachari, K.; Rendell, A.; Burant, J. C.; Iyengar, S. S.; Tomasi, J.; Cossi, M.; Rega, N.; Millam, J. M.; Klene, M.; Knox, J. E.; Cross, J. B., et al. Gaussian09 Revision D.01., Gaussian Inc. Wallingford CT 2009.

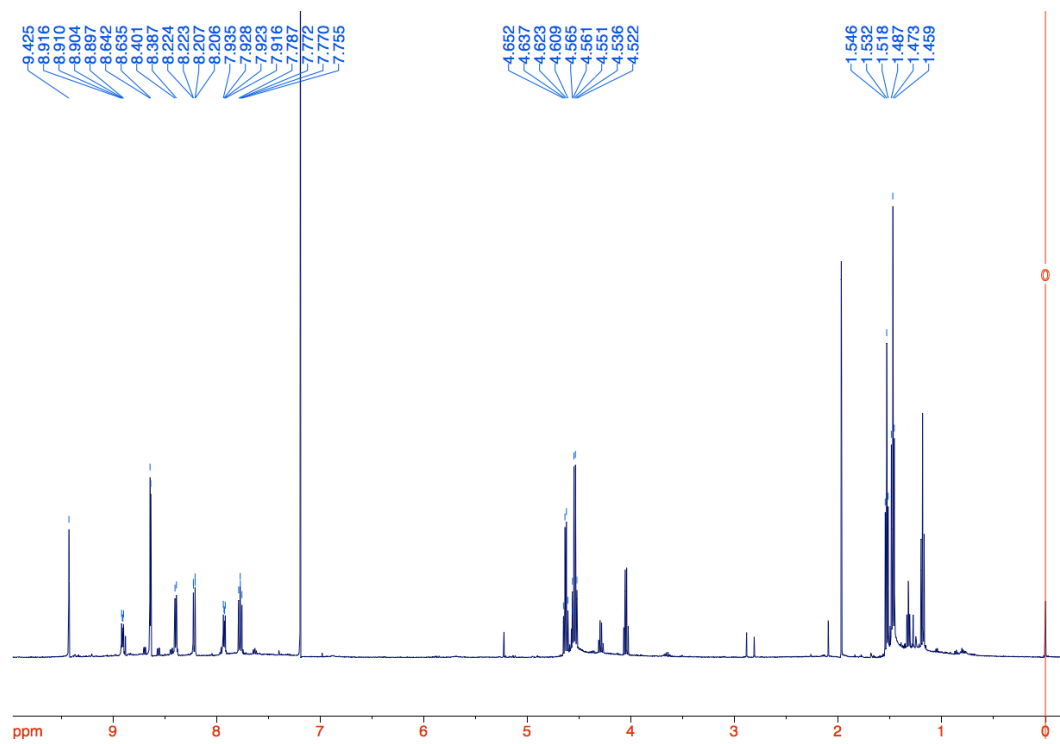
<sup>2</sup> F. Alonso, Y. Moglie, G. Radivoy and M. Yus, *Eur. J. Org. Chem.* **2010**, 10, 1875

mmol) in ether (250 mL) at  $-55\text{ }^{\circ}\text{C}$  under a  $\text{N}_2$  atmosphere. The addition complete the reaction stirred for 20 min at this temperature and was then warmed to  $35\text{ }^{\circ}\text{C}$  and stirred for 1 hr more. The reaction mixture was then cooled to  $-75\text{ }^{\circ}\text{C}$  and DMF (6.0 mL, 78 mmol) was added. The reaction mixture was allowed to warm to room temperature, stirred overnight and was then quenched with water. A majority of the solvent was removed in vacuo and the product was precipitated with water. The product was filtered, rinsed with water and then purified by column chromatography using a gradient of 100% hexane to 100% chloroform to afford bright orange crystals (2.4 g, 54% yield). NMR data was in agreement with literature.<sup>3</sup>  $^1\text{H}$  NMR ( $\text{CDCl}_3$ , 500 MHz,  $25\text{ }^{\circ}\text{C}$ )  $\delta$  11.51 (s, 2H), 8.77 (dd,  $J = 6.9, 3.3\text{ Hz}$ , 4H), 7.73 (dd,  $J = 6.9, 3.3\text{ Hz}$ , 4H).  $^{13}\text{C}$  NMR ( $\text{CDCl}_3$ , 125 MHz,  $25\text{ }^{\circ}\text{C}$ )  $\delta$  194.3, 131.8, 130.2, 128.4, 124.2.

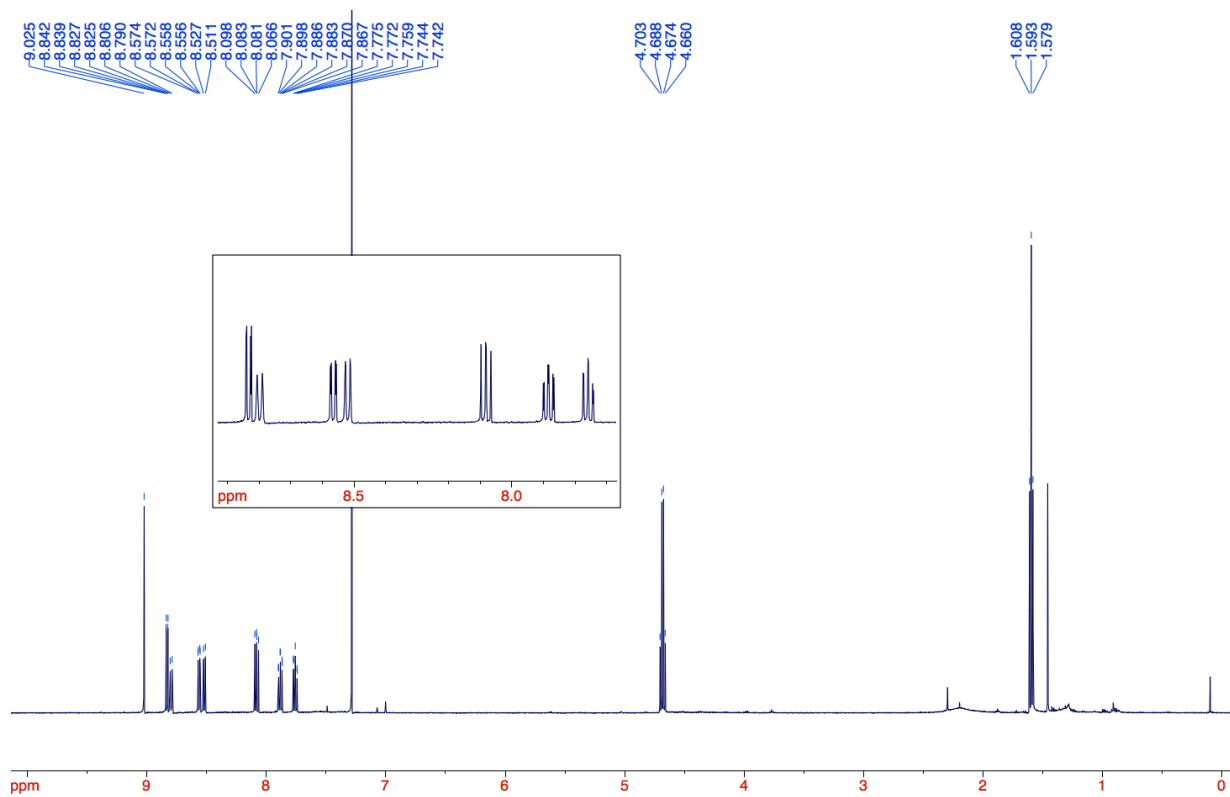


$^1\text{H}$  NMR spectrum of **5** (bottom) and a mixture of **5** and the azirine intermediate (top) in  $\text{CDCl}_3$ .

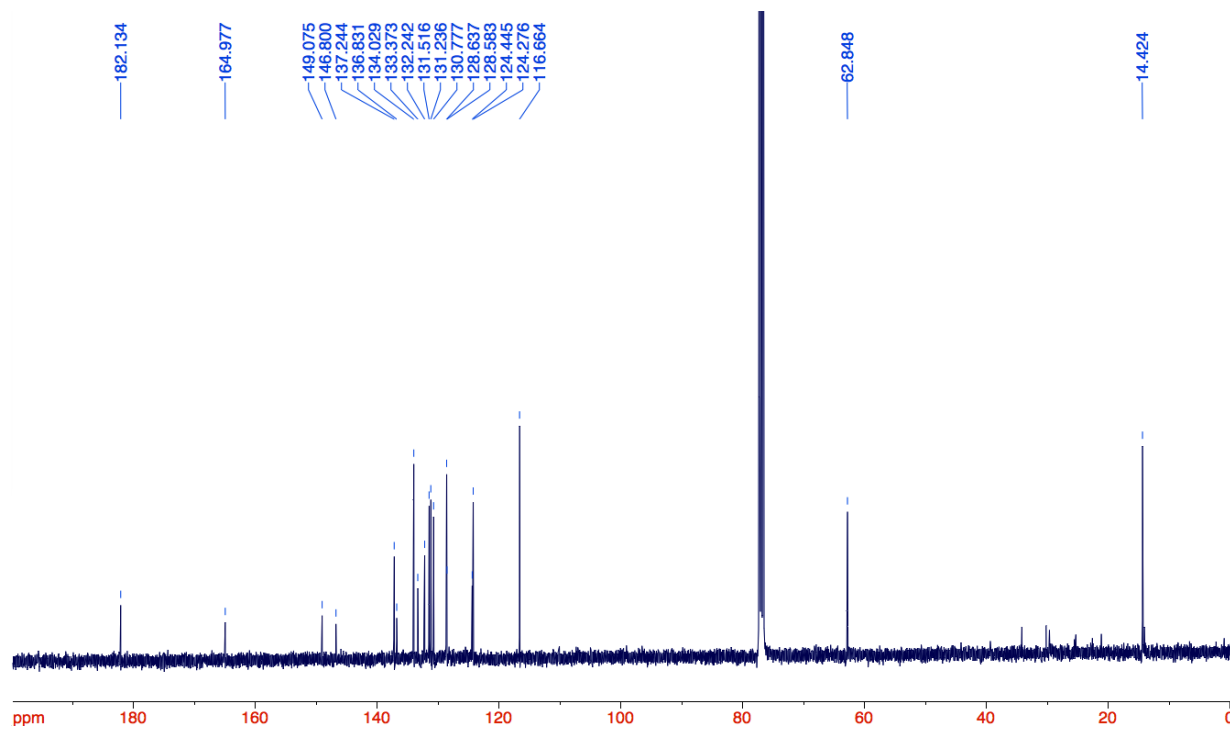
<sup>3</sup> A. Lee, M. Grace, A. Meyer and K. Tuck, *Tetrahedron Letters*, **2010**, *51*, 1161



$^1\text{H}$  NMR spectrum of crude compounds **6** and **7** in  $\text{CDCl}_3$ .

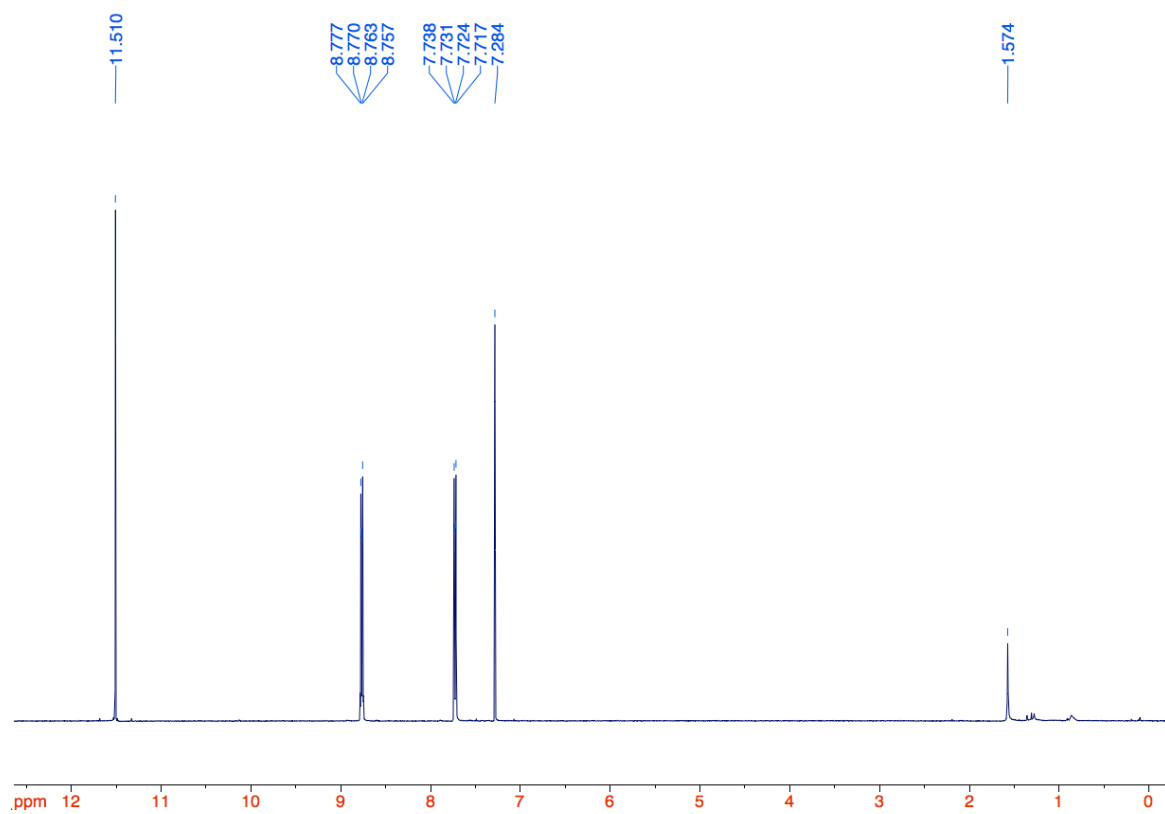


$^1\text{H}$  NMR spectrum of compound **3** in  $\text{CDCl}_3$ .

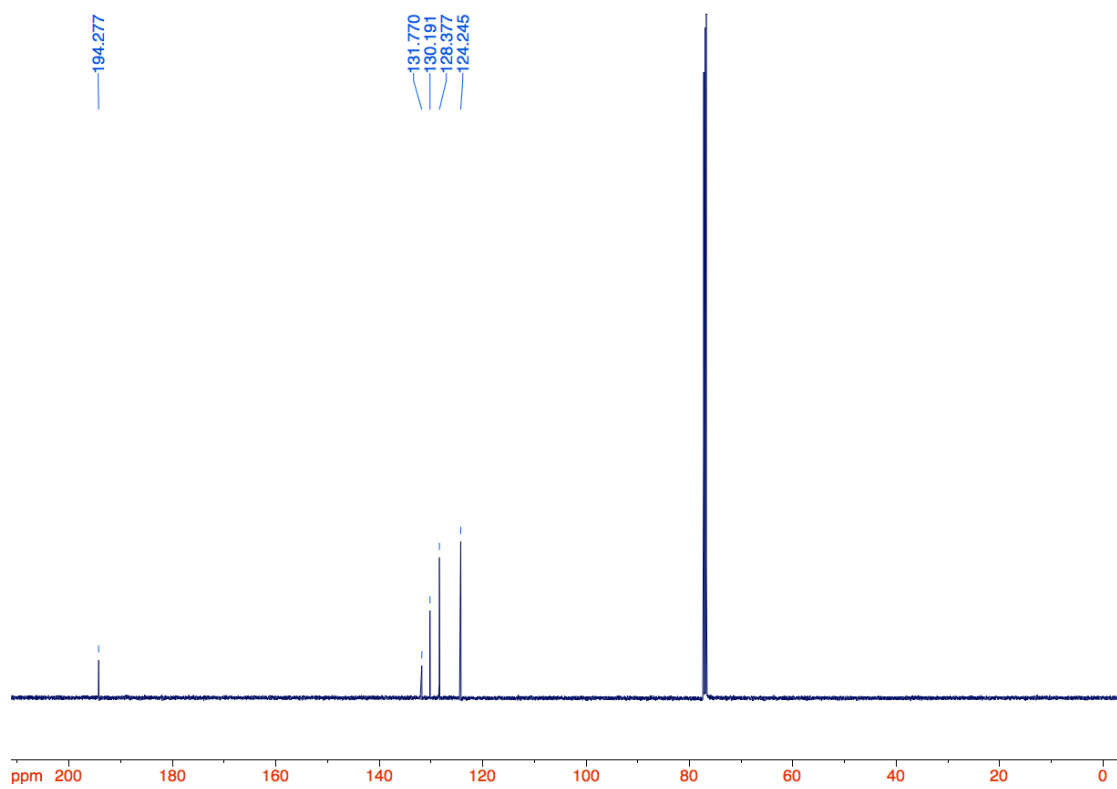


$^{13}\text{C}$  NMR spectrum of compound **3** in  $\text{CDCl}_3$ .

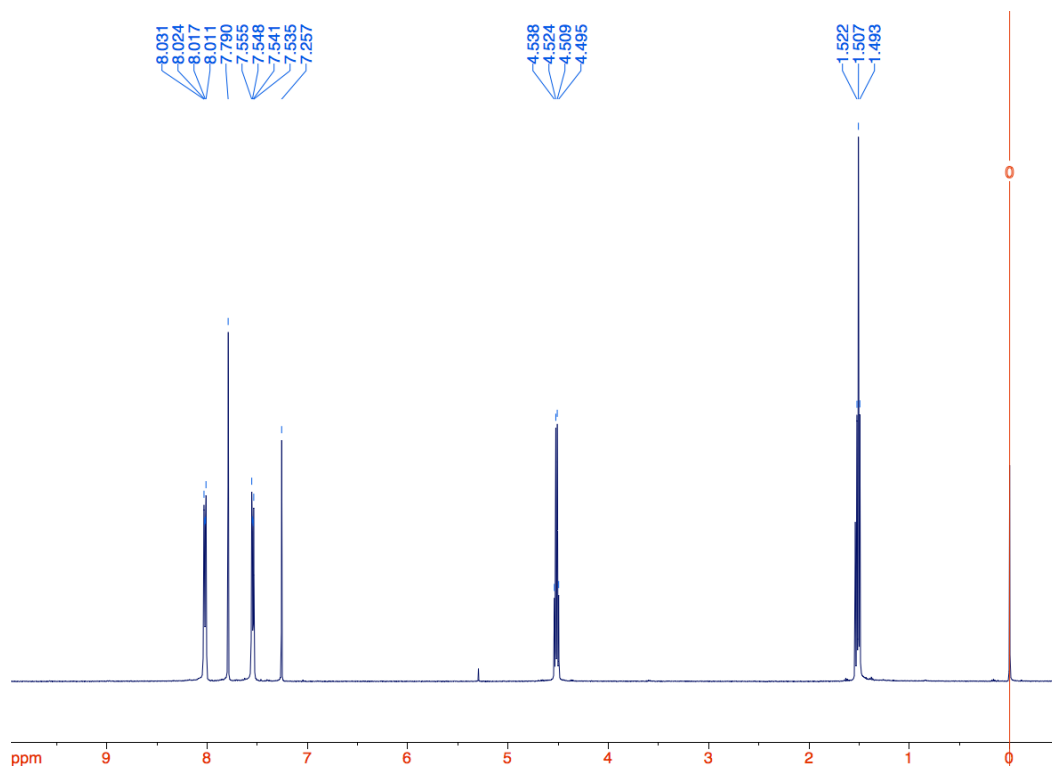




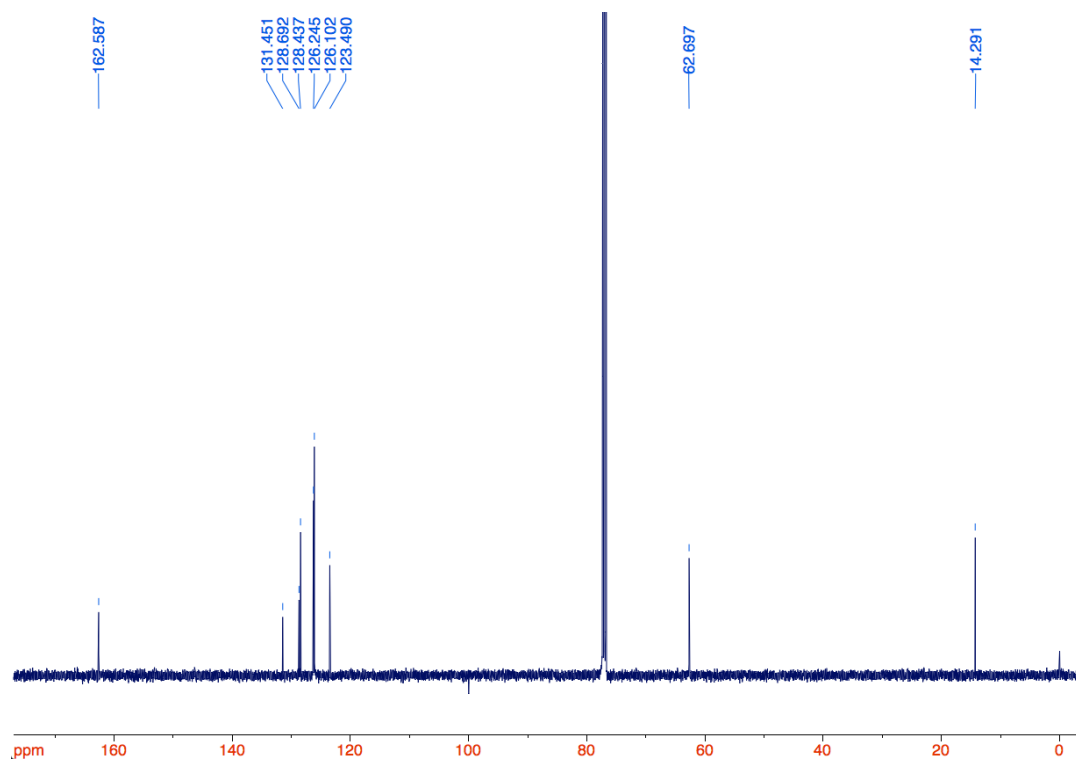
<sup>1</sup>H NMR spectrum of compound **4** in CDCl<sub>3</sub>.



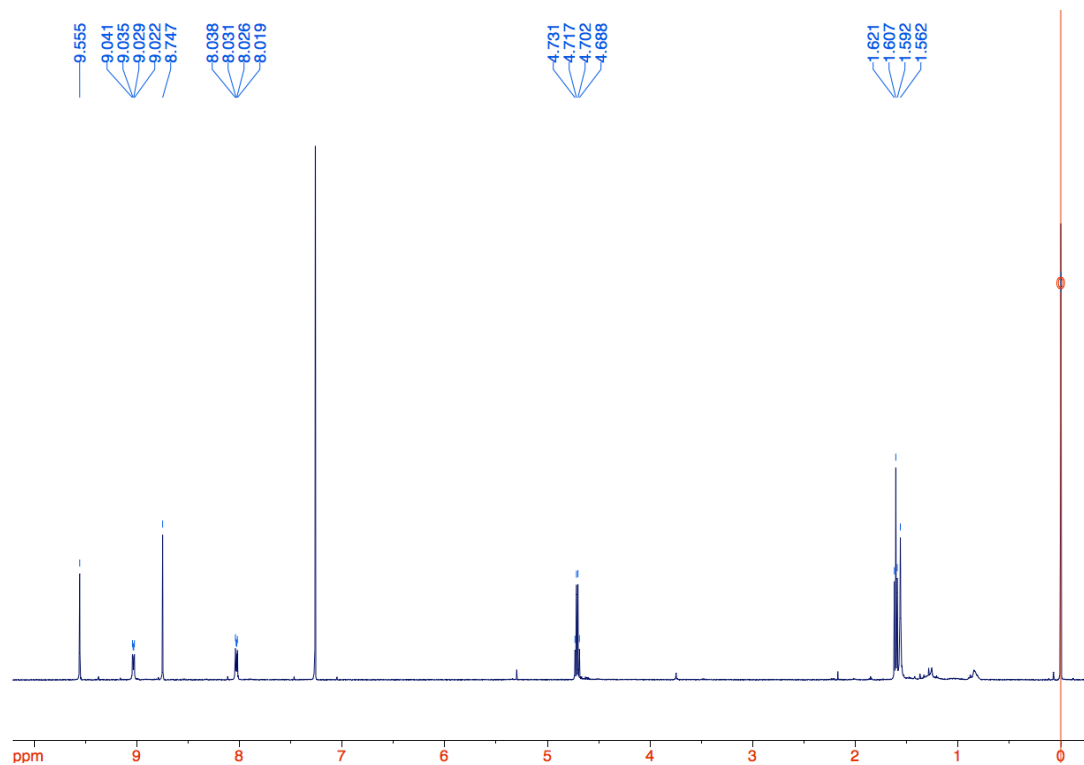
<sup>13</sup>C NMR spectrum of compound **4** in CDCl<sub>3</sub>.



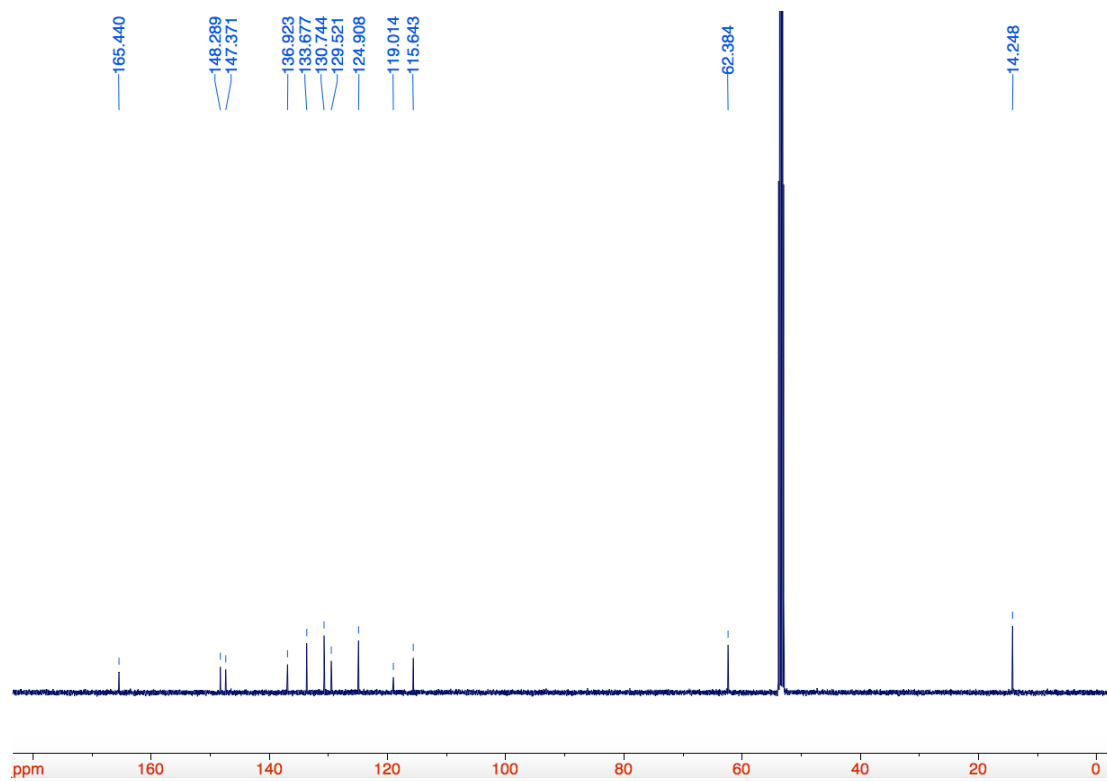
<sup>1</sup>H NMR spectrum of compound 5 in CDCl<sub>3</sub>.



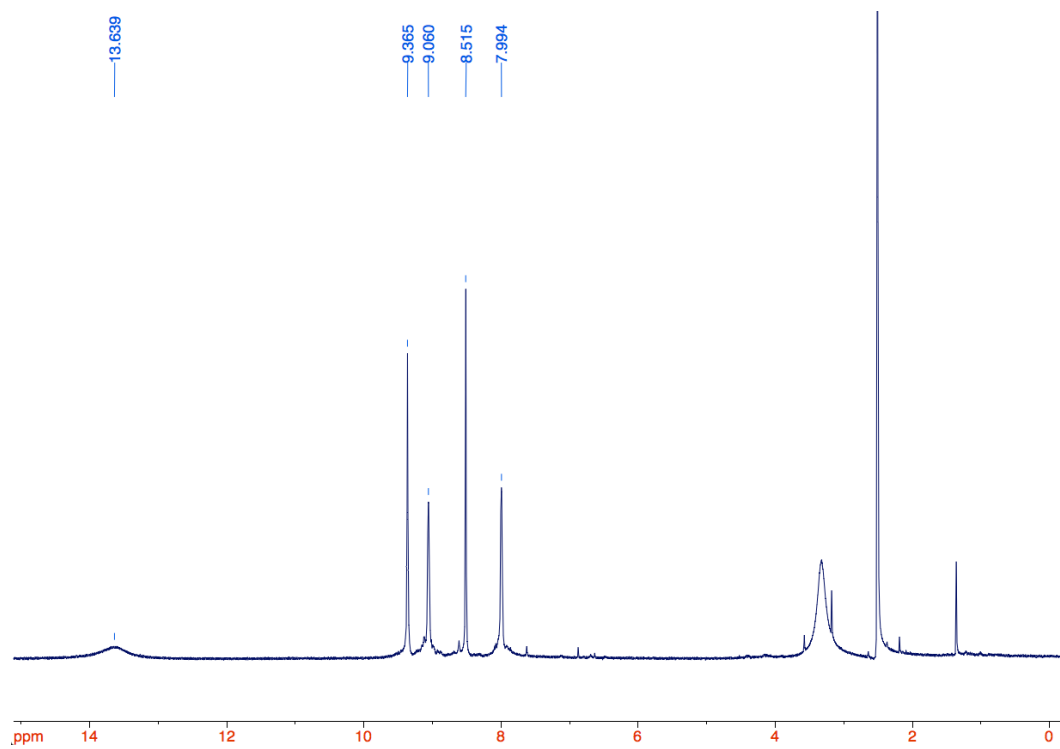
<sup>13</sup>C NMR spectrum of compound 5 in CDCl<sub>3</sub>.



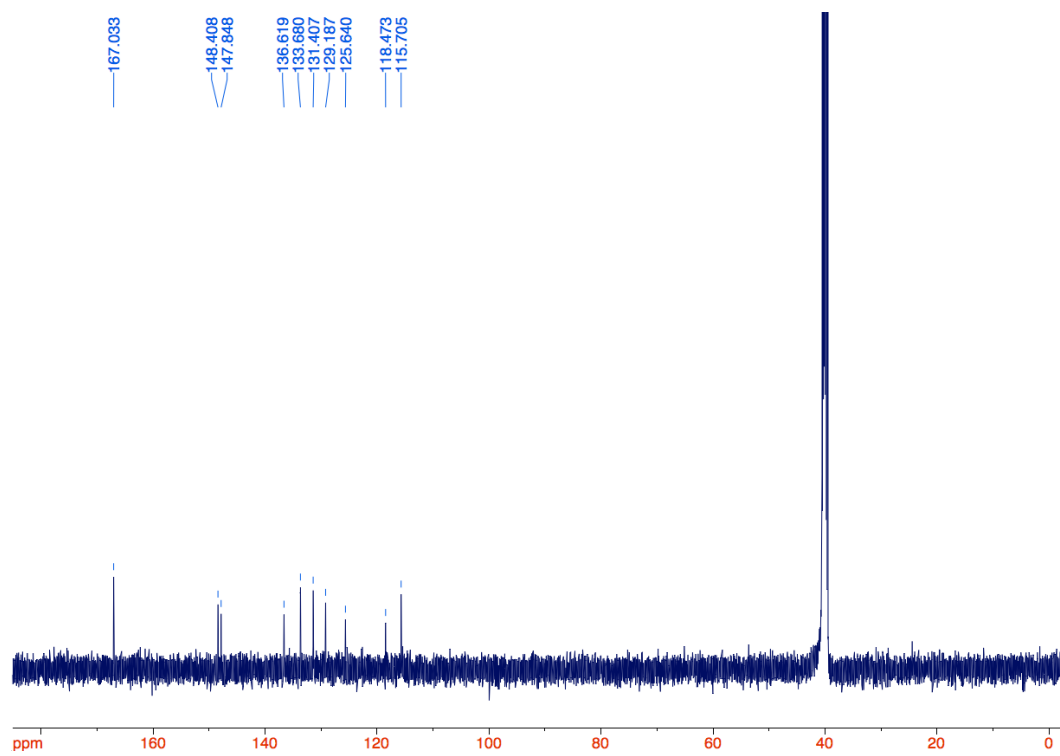
$^1\text{H}$  NMR spectrum of compound **6** in  $\text{CDCl}_3$ .



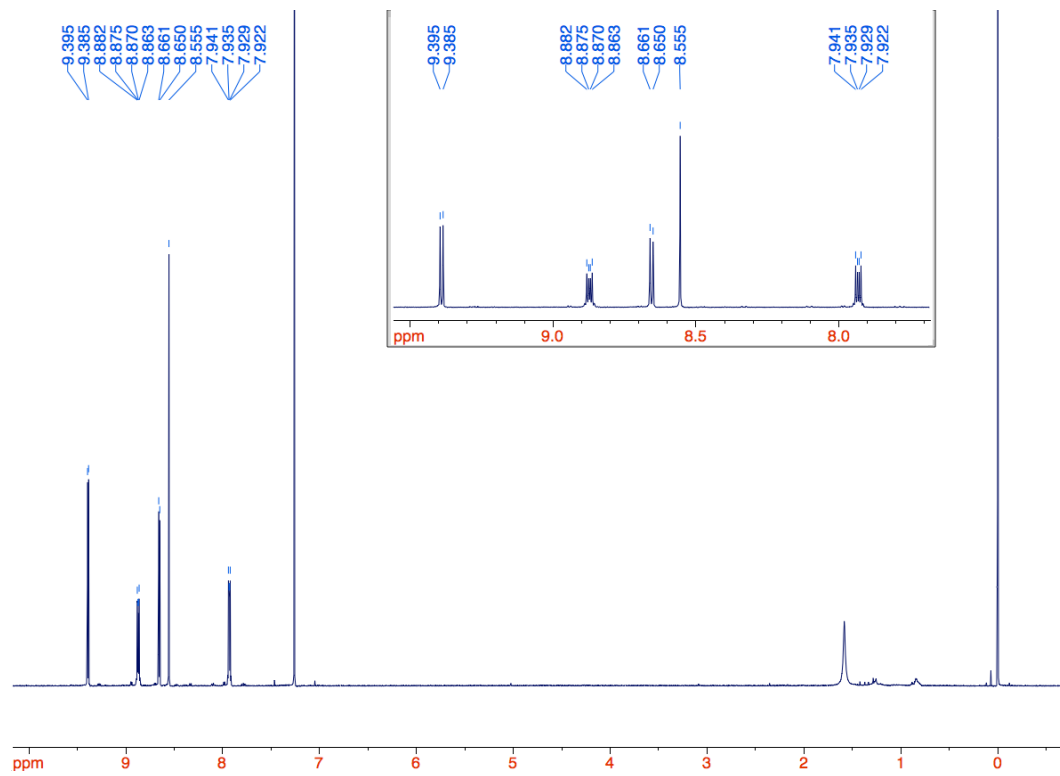
$^{13}\text{C}$  NMR spectrum of compound **6** in  $\text{CDCl}_3$ .



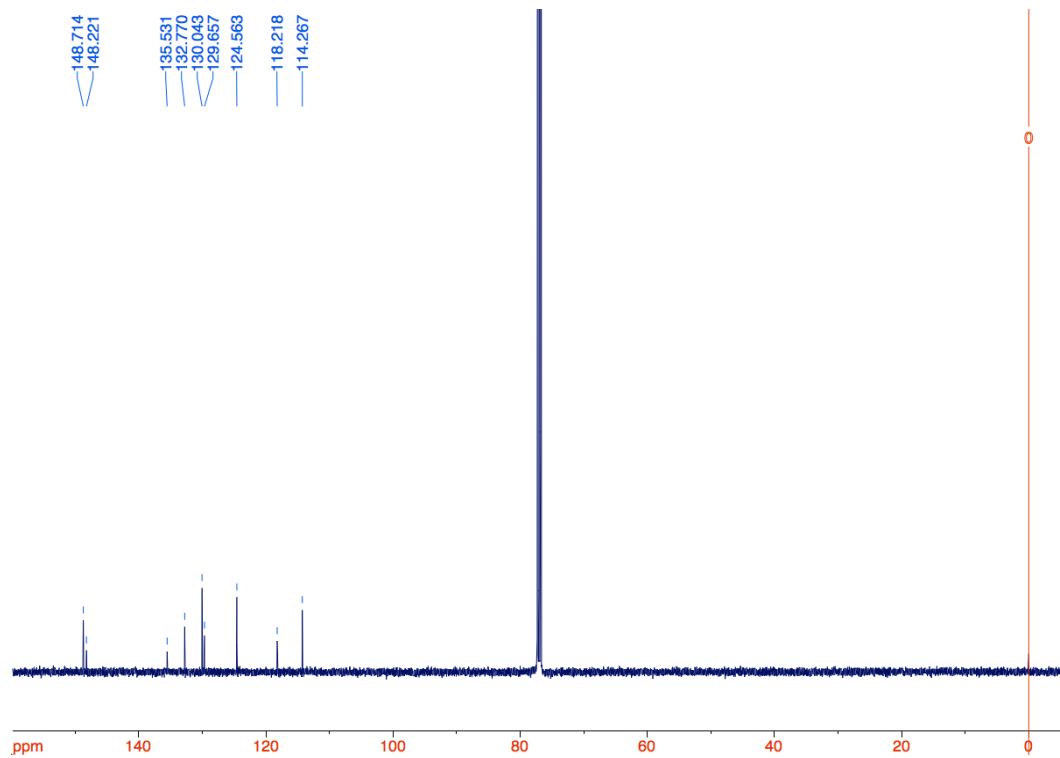
$^1\text{H}$  NMR spectrum of compound **8** in  $(\text{CD}_3)_2\text{SO}$ .



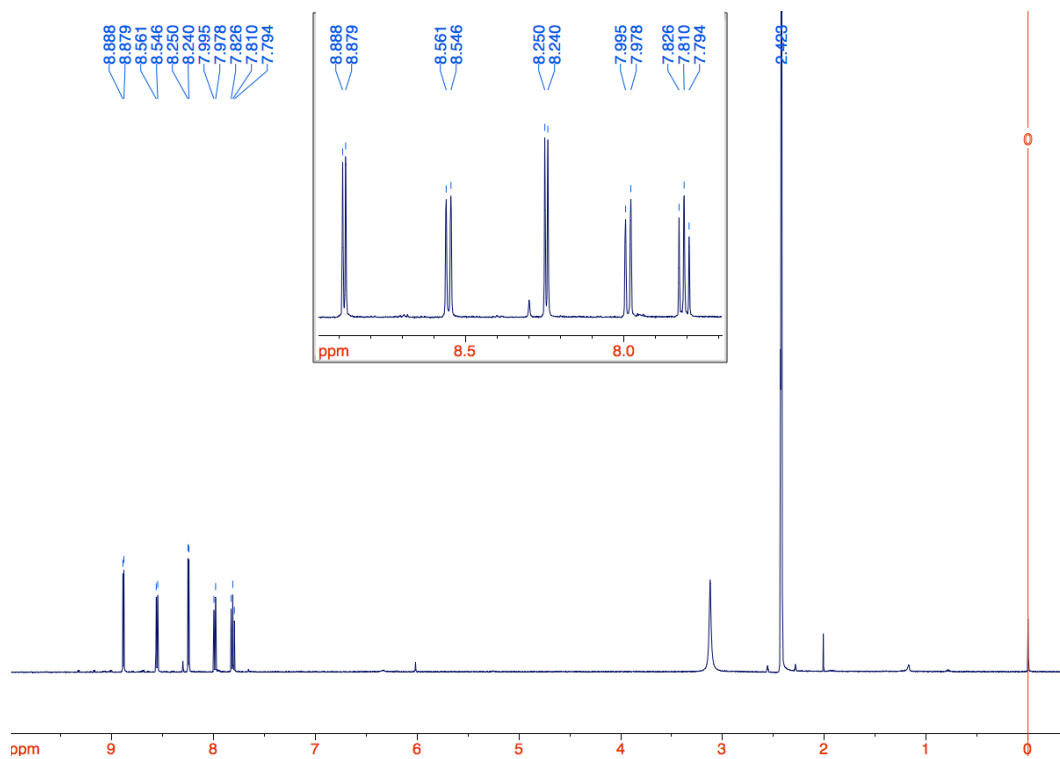
$^{13}\text{C}$  NMR spectrum of compound **8** in  $(\text{CD}_3)_2\text{SO}$ .



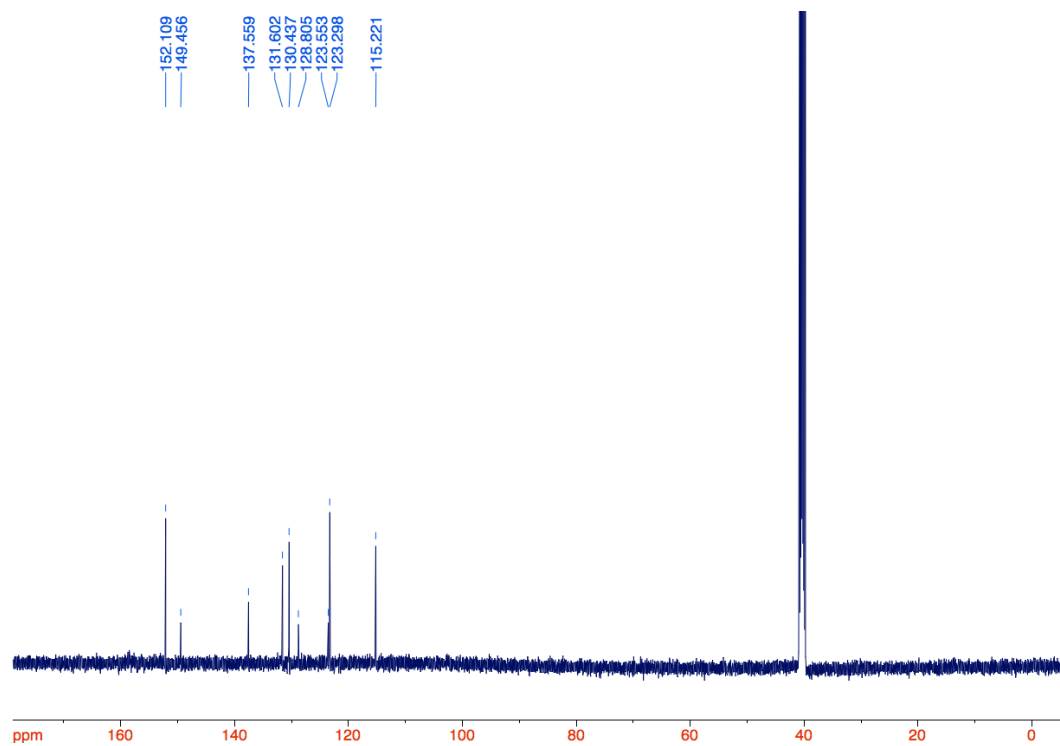
<sup>1</sup>H NMR spectrum of compound **10** in CDCl<sub>3</sub>.



<sup>13</sup>C NMR spectrum of compound **10** in CDCl<sub>3</sub>.

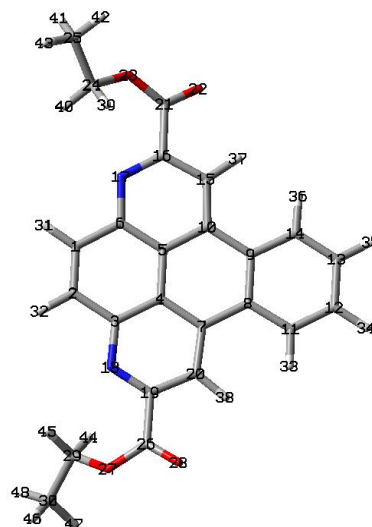
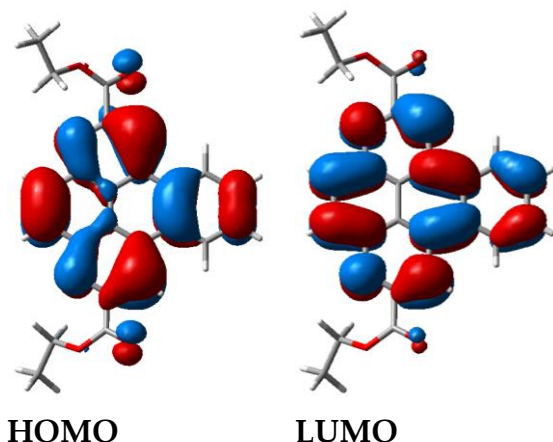


$^1\text{H}$  NMR spectrum of compound **11** in  $(\text{CD}_3)_2\text{SO}_3$  at  $50\text{ }^\circ\text{C}$ .



$^{13}\text{C}$  NMR spectrum of compound **11** in  $(\text{CD}_3)_2\text{SO}_3$  at  $70\text{ }^\circ\text{C}$ .

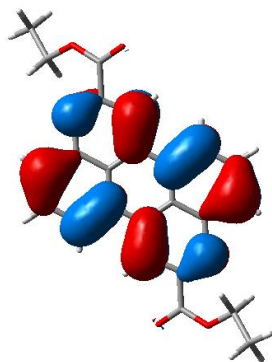
Computational data for 6 (SCF total energy = - 1335.86041416 hartrees)



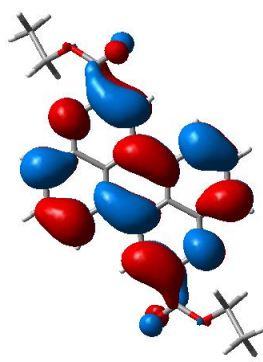
Coordinates (Angstroms)			
Atom	X	Y	Z
1	0.355116	4.340952	-0.12501
2	0.355071	3.003521	0.125481
3	1.587289	2.274221	0.260092
4	2.822883	2.971544	0.132033
5	2.822931	4.372699	-0.13191
6	1.587383	5.070137	-0.2598
7	4.041362	2.255358	0.271962
8	5.312964	2.973243	0.134742
9	5.313012	4.37077	-0.13494
10	4.041459	5.088772	-0.272
11	6.547967	2.306575	0.263234
12	7.749045	2.98392	0.132543
13	7.749092	4.359866	-0.13304
14	6.54806	5.037323	-0.26359
15	3.937998	6.453721	-0.54235
16	2.673515	7.054846	-0.6342
17	1.522845	6.395281	-0.49779
18	1.522663	0.949082	0.498092
19	2.673288	0.289395	0.634311
20	3.937809	0.890418	0.542326
21	2.649412	8.525387	-0.99507
22	3.582597	9.013025	-1.5988
23	1.596208	9.300299	-0.68235
24	0.573762	8.966967	0.287952

25	-0.03262	10.2816	0.747372
26	2.649136	-1.18113	0.995279
27	1.596	-1.95614	0.682527
28	3.582227	-1.66868	1.599226
29	0.573759	-1.62321	-0.28813
30	-0.03237	-2.93804	-0.7473
31	-0.5672	4.90299	-0.23142
32	-0.56729	2.441571	0.232023
33	6.566333	1.242299	0.468618
34	8.687027	2.44637	0.236595
35	8.687111	4.897329	-0.23721
36	6.5665	6.101597	-0.46897
37	4.802166	7.08402	-0.70472
38	4.80194	0.260044	0.704595
39	1.01896	8.419612	1.124042
40	-0.16553	8.317818	-0.1845
41	-0.45633	10.82926	-0.10024
42	0.721624	10.91553	1.223954
43	-0.83359	10.08814	1.469883
44	1.019089	-1.07606	-1.12428
45	-0.16573	-0.974	0.18394
46	-0.45622	-3.4855	0.10037
47	0.722055	-3.57204	-1.22352
48	-0.83319	-2.74489	-1.47006

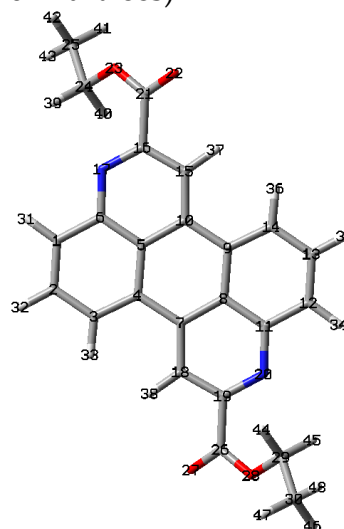
Computational data for 7 (SCF total energy = -1335.85071464 hartrees)



HOMO



LUMO

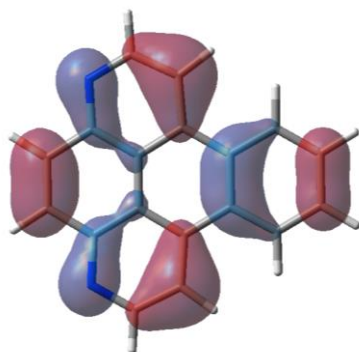


Atom	Coordinates (Angstroms)		
	X	Y	Z
1	-0.54369	5.89812	-1.88808
2	-1.18043	4.680904	-1.79265
3	-0.46009	3.521464	-1.44651
4	0.905833	3.56405	-1.19111
5	1.582661	4.818744	-1.28408
6	0.849075	5.993931	-1.63914
7	1.683983	2.369097	-0.82357
8	3.084294	2.498386	-0.56607
9	3.761106	3.753096	-0.65895
10	2.982988	4.948021	-1.02664
11	3.817881	1.323197	-0.21101
12	5.210616	1.41904	0.038097
13	5.847318	2.636289	-0.05715
14	5.126989	3.795722	-0.40333
15	3.534181	6.21449	-1.13305
16	2.725563	7.310447	-1.51028
17	1.431248	7.220034	-1.75694
18	1.132834	1.102586	-0.71741
19	1.941461	0.006623	-0.34022
20	3.235737	0.097068	-0.09337
21	3.400796	8.666644	-1.53625
22	4.394011	8.854531	-0.86422
23	2.905568	9.67895	-2.26817

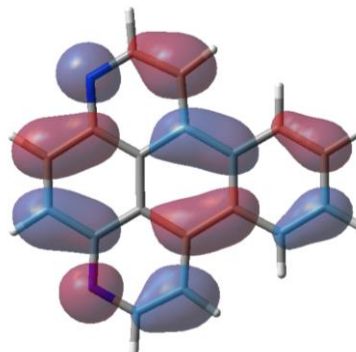
24	1.924876	9.547037	-3.32651
25	2.071151	10.77579	-4.20711
26	1.266307	-1.34962	-0.31447
27	0.273507	-1.53766	-0.98706
28	1.760968	-2.36172	0.418133
29	2.741719	-2.22965	1.47641
30	2.595677	-3.45842	2.35701
31	-1.07481	6.806994	-2.15112
32	-2.24686	4.604697	-1.98357
33	-0.99739	2.581799	-1.38001
34	5.741742	0.510167	0.30114
35	6.913715	2.712528	0.133946
36	5.664256	4.735413	-0.46968
37	4.576179	6.415348	-0.9218
38	0.09087	0.901719	-0.92882
39	0.930582	9.477119	-2.88229
40	2.108414	8.627682	-3.89023
41	3.071867	10.8256	-4.64757
42	1.904456	11.68927	-3.62778
43	1.334316	10.74034	-5.01754
44	2.558047	-1.31032	2.040141
45	3.735967	-2.15957	1.032126
46	2.762549	-4.37188	1.77769
47	1.59497	-3.50842	2.797468
48	3.332507	-3.42282	3.167438



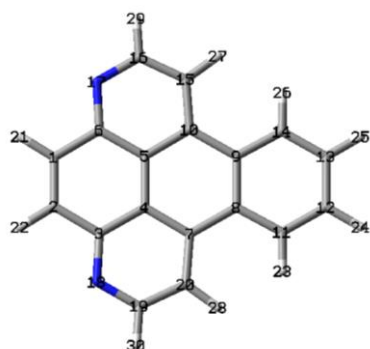
Computational data for 10 (SCF total energy = -801.49470624 hartrees)



HOMO



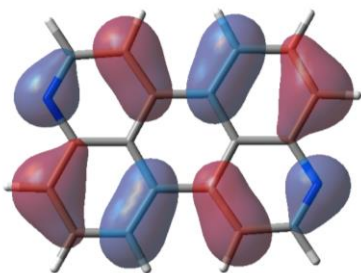
LUMO



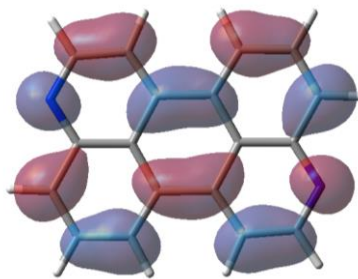
Atom	Coordinates (Angstroms)		
	X	Y	Z
1	0.360105	4.340085	-0.12981
2	0.360061	3.004383	0.130268
3	1.591057	2.274855	0.272459
4	2.827471	2.971258	0.136638
5	2.827518	4.372984	-0.1365
6	1.591149	5.0695	-0.27216
7	4.044994	2.254719	0.276678
8	5.316018	2.973495	0.136271
9	5.316065	4.370518	-0.13646
10	4.045088	5.08941	-0.2767
11	6.552973	2.309317	0.266157
12	7.754935	2.984262	0.134163
13	7.75498	4.359527	-0.13467
14	6.553063	5.034582	-0.26651
15	3.937815	6.45785	-0.54396

16	2.674087	7.045562	-0.65828
17	1.521173	6.392667	-0.53027
18	1.520992	0.951694	0.530578
19	2.673864	0.298693	0.65843
20	3.937631	0.886289	0.543951
21	-0.56076	4.904024	-0.23964
22	-0.56084	2.440528	0.240221
23	6.572254	1.24544	0.474655
24	8.692873	2.446443	0.239355
25	8.692954	4.89726	-0.23999
26	6.572414	6.098458	-0.47501
27	4.81356	7.084802	-0.66668
28	4.813334	0.259256	0.666554
29	2.597262	8.111749	-0.86658
30	2.596968	-0.76749	0.866742

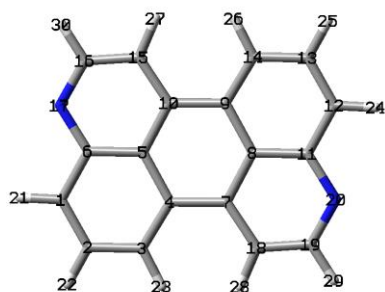
Computational data for 11 (SCF total energy = -801.4849891 hartrees)



HOMO



LUMO



Coordinates (Angstroms)			
Atom	X	Y	Z
1	-0.54084	5.903049	-1.88672
2	-1.17752	4.685184	-1.7998
3	-0.4582	3.524972	-1.45458
4	0.906223	3.566647	-1.19183
5	1.583091	4.823414	-1.27746
6	0.850078	6.001253	-1.62853
7	1.682894	2.369373	-0.82882
8	3.083865	2.49372	-0.57268
9	3.76073	3.75049	-0.65829
10	2.984066	4.947758	-1.02134
11	3.816879	1.315881	-0.22161
12	5.20779	1.414091	0.036616
13	5.844466	2.631962	-0.05027
14	5.125141	3.792173	-0.3955

15	3.533746	6.217544	-1.13391
16	2.719447	7.311662	-1.48666
17	1.425565	7.234165	-1.72986
18	1.133223	1.099579	-0.71629
19	1.947524	0.00546	-0.36355
20	3.241398	0.082962	-0.12031
21	-1.06854	6.813796	-2.15031
22	-2.2431	4.609249	-1.99728
23	-0.99635	2.584944	-1.39656
24	5.735493	0.503344	0.300214
25	6.910032	2.707903	0.147251
26	5.663286	4.732206	-0.45349
27	4.588213	6.396071	-0.95558
28	0.078763	0.921046	-0.89465
29	1.499438	-0.98424	-0.27939
30	3.16754	8.30135	-1.57086